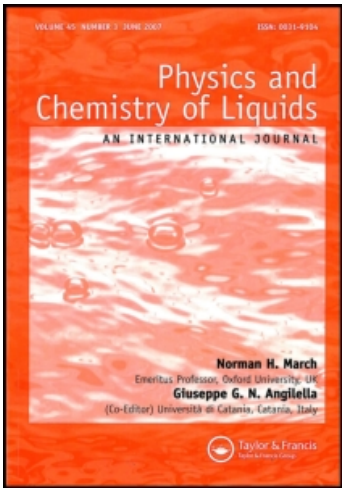

Physics and Chemistry of Liquids
Publication details, including instructions for authors and subscription information:
http://www.informaworld.com/smpp/title~content=t713646857

Isotope Effects in Liquid Metals

M. Ginoza[a]; N. H. March[a]
[a] Theoretical Chemistry Department, University of Oxford, Oxford, England

To cite this Article Ginoza, M. and March, N. H.(1985) 'Isotope Effects in Liquid Metals', Physics and Chemistry of Liquids, 15: 2, 75 — 111
To link to this Article: DOI: 10.1080/00319108508078471
URL: http://dx.doi.org/10.1080/00319108508078471

Phys. Chem. Liq., 1985, Vol. 15, pp. 75–112
0031-9104/85/1502-0075$18.50/0

Printed in the United Kingdom

Review Article

Isotope Effects in Liquid Metals

M. GINOZA and N. H. MARCH

Theoretical Chemistry Department, University of Oxford, 1 South Parks Road, Oxford OX1 3TG, England.

(*Received March 27, 1985*)

The areas treated in this article are:

(i) The Haeffner effect; where the light isotope moves towards the anode in all cases so far investigated.

(ii) Self diffusion and mutual diffusion.

(iii) Shear viscosity of pure isotopes of Li^6 and Li^7.

In the course of the discussion, the Haeffner effect is shown to be directly related to electrical resistivity at the level of the lowest order Born approximation.

Models used for treating isotopic mass effects are then considered; limitations and usefulness being assessed by comparison with experimental data on liquid metals. The marked contrast with low temperature isotope effects is finally commented on.

1 INTRODUCTION

Isotope effects are known to exist in liquid metals from a variety of experiments with light isotopes, and in particular with Li^6 and Li^7. Some striking, and surprising, regularities exist more generally, especially the effect discovered by Haeffner.[1] Here, in an applied electric field, the light isotope in the isotopic liquid metal mixture is found, invariably, to move towards the anode. No known exceptions to this rule exist. The problem of electromigration is closely related, but presumably the understanding of the Haeffner effect is an essential prerequisite to an understanding of this phenomenon. For a detailed review on electromigration, the article by Huntington[2] may be consulted.

The purpose of the present article is two-fold. First, in Sections 2–4 below, the facts, and some basic phenomenology, are presented in turn for

(i) the Haeffner effect, (ii) self and mutual diffusion and (iii) shear viscosity. Following this, Sections 5 and 6 are concerned with microscopic theory. In particular, in Section 5 the theory underlying the Haeffner effect is presented, in lowest order Born approximation, in a form in which it is directly related to electrical resistivity. From this theory, it clearly emerges, within the lowest order Born approximation, that the condition for the Haeffner effect places clear constraints on the electrical resistivities associated with different isotopes. But to explain the resulting inequality there is, as yet, no unambiguous and generally accepted mechanism. Therefore Section 6 concerns itself with some models in which isotope effects are explicitly introduced. These start from the very simple problem of a single valence-electron atom in motion which then suggests a Hamiltonian with particular mass scaling properties whose consequences can be worked out. This is followed by a discussion of a model of Rezayi and Suhl[3] which, though devised particularly with solids in mind, may have interesting consequences for the liquid state. The relation of this model to collective modes in liquids, and in liquid metal isotopic mixtures, is briefly considered.

In the final section, the limitations, and the usefulness of the various models is discussed in relation to the experimental facts. While there seems as yet, no microscopic theory which can embrace all the experimental facts, it emerges that electronic and atomic transport are inextricably linked in liquid metals. For situations where there are light isotopes present, it does seem that present evidence supports the existence of the liquid counterpart of the 'local mode' round an impurity in solid state language. However, this cannot be the explanation of the shear viscosity measurements. Therefore, finally, the dynamic interaction between ions in liquid metals is discussed, and some further experiments are proposed which may shed light on the fundamental problems remaining in this area.

2 HAEFFNER EFFECT

The fact that, when an electric field is applied to an isotopic liquid metal mixture, the light isotope diffuses towards the anode was discovered by Haeffner. Short reviews to which the reader is referred are those of Epstein,[4] and of Faber.[5] There appear to be no known exceptions to this rule, and therefore it seems clear that the answer should not depend on the fine detail of liquid metal theory.

Though the Haeffner effect is our prime interest here, it is useful to regard this effect as a special case of the more general electromigration problem in liquid metal alloys. This is the effect found in a number of binary metal alloys, where the constituent ions drift in opposite directions under the

influence of an applied dc electric field. This effect, known alternatively as electrotransport or electrodiffusion, has generally been explained in terms of a competitive transfer of momentum from the conduction electron current to the two species of ions in the alloy, as discussed, for example, by Landauer and Woo.[6]

The force acting on each ion is assumed to be the sum of two components:

i) a direct force due to the applied electric field itself, which tends to drive the ion towards the cathode, and

ii) an 'electron drag' component arising from the scattering of conduction electrons by the ion, which acts to pull the ions towards the anode; that is in the same direction as the electron current. The ionic species which experiences the greater electron drag will then presumably migrate towards the anode, while the other, in order not to build up density gradient, will migrate in the opposite direction.

One should be cautious, as Stroud[7] points out, because, so far, the attempts have been largely focussed on calculating a force rather than a current. The ionic current induced in the liquid binary alloys under discussion depends on an ionic mobility as well as a driving force. If the local fluctuations in the drag force are not too large, it should be possible to obtain an ionic mass current by simply multiplying the average driving force by an average mobility. Stroud's work,[7] however, suggests that these fluctuations are substantial. They should therefore be taken into account in a quantitative theory of electromigration.

To press the above points in the alloy, before specializing to the Haeffner effect, Stroud, in his work on the average driving force for electromigration in liquid metal alloys concludes that there is a correlation between the calculated driving force acting on a solute ion and its assumed hard sphere diameter. He says 'in virtually every case it is found that the effective valence of the solute atom becomes more negative as the assumed hard-sphere diameter decreases, i.e. the smaller the atom, the more likely it is to migrate to the anode.'

However, he then goes on to point out that the correlation between the driving force and hard-sphere diameter reflects a sensitivity of the driving force to the structure factors, i.e. to the local environment of the solute ion. He notes, in particular, that the sensitivity to the local environment ultimately arises from quantum-mechanical interference between the electron wave scattered off the ion on which a force is being exerted and the wave scattered off a neighbouring ion. The recoil of the ion induced by this scattered wave gives rise to the electron drag force. Although such sensitivity to environment is to be expected, the reason for the direction of the correlation; i.e. large drag forces corresponding to small diameter, is difficult to

pinpoint. He then observes that since this environment is likely to fluctuate in a liquid, this sensitivity suggests that the driving forces may also experience substantial local fluctuations, which are likely to correlate with local fluctuations in solute mobility. Such correlated fluctuations have long been thought necessary to account for electric field induced isotope separations, i.e. the Haeffner effect we are primarily concerned with here.

So far, we do not have a theory of such sophistication. However, in a later section, we shall consider a treatment, due to Parrinello, Tosi and March,[8] in which the direction of ion flow is directly related, in the liquid metal isotopic mixture, to the 'partial resistivities' of the component isotopes.

2.1 Thermotransport

The process in which a concentration gradient is induced by a temperature gradient in solids, liquids or gases has been called thermotransport, thermomigration, thermal diffusion or the Ludwig–Soret effect. The phenomenon, while well studied in many materials, as reviewed by Grew[9] and by Huntington, has been less extensively studied in liquid metals.

In a typical experimental set-up, a liquid with atomic fraction x_1 of component 1 is contained in a vertical capillary several cm long. It is then subjected to a temperature gradient of 1–5 C/mm for a time $t \sim l^2/2D$. D denoting the diffusion constant, so that a steady-state concentration profile is developed. For liquid metals, the customary practice is to express the results in terms of the net heat of transport Q^*, which for dilute alloys is given by

$$\frac{\mathrm{d}(\ln x_1)}{\mathrm{d}(1/T)} = \frac{Q^*}{R}.$$

Evidently, Q^* is then obtained directly from a plot of $\ln x_1$ versus $1/T$.

It is worthy of note first that Gonzales and Oriani[10] have pointed out that a strong correlation exists between Q^* in solid metal systems and the effective valence measured in electrotransport experiments. This is expected, according to the arguments of Gerl,[11] if the electron contribution to Q^* is dominant. The correlation is particularly good for dilute liquid metals, in which the component which migrates to the hot end in thermotransport is the one which goes to the anode in electrotransport. Particularly important in the present context is that it holds for the isotopes of Li, since the migration of ^{6}Li to the hot end is consistent with the measured Haeffner effect, according to Ott and Lunden[12] and to Verhoeven.[13]

Even with the large positive temperature gradients that are generally used for these experiments, Rigney[14] emphasizes that convection can develop

during thermotransport if the component that migrates to the hot end has a higher density than the other component. The work of Bhat and Swalin[15] should also be referred to in this connection.

3 DIFFUSION OF IONS IN LIQUID METALS

From the outline of the Haeffner effect given above, we turn to the closely related subject of isotope effects in diffusion. Here, following the pioneering experiment of Ban *et al.*[16] on the shear viscosity of pure isotopes Li^6 and Li^7, to be summarized in the following section, diffusion measurements have been carried out, using nuclear magnetic resonance techniques, by Murday and Cotts[17] and by Kruger *et al.*[18]

It should be noted at this point that, of the two major methods presently available, namely nuclear magnetic resonance (NMR) and radioactive tracer methods, NMR alone can measure genuine self-diffusion, whereas the tracer technique evidently gives results characteristic of an isotopic mixture. Thus we shall begin with the NMR results, and their interpretation at a phenomenological level. Then we shall add a brief account of radioactive tracer measurements.

3.1 NMR results

Murday and Cotts[17] measured the liquid state self-diffusion coefficients of Li^6 and Li^7 in isotopically enriched Li^6 and Li^7 metal and in several isotopic alloys by the nuclear magnetic resonance spin echo, pulsed magnetic gradient technique. At the melting point of 180–5°C, they determined the self-diffusion coefficients as

$$D_m^6 = (6.8 \pm 0.7) \times 10^{-5} \text{ cm}^2/\text{sec}$$

for Li^6 in 99% Li^6 and

$$D_m^7 = (5.8 \pm 0.6) \times 10^{-5} \text{ cm}^2/\text{sec}$$

for Li^7 in 99.9% Li^7.

They note that the ratio of these measured values (1.18 ± 0.07) is greater than the square root of the mass ratio $(M^7/M^6)^{1/2} = 1.08$.

Furthermore, the isotopic ratio of self-diffusion coefficients is observed to be less than the ratio of the mutual diffusion coefficients in almost pure Li^6 and almost pure Li^7, $(D_{Mm}^6/D_{Mm}^7) = 1.35$ and the viscosity ratio discussed further below: $\eta^7/\eta^6 = 1.44$. They observe that the dependence of D on isotopic alloy concentration appears to be relatively weak and linear in all but the very low concentrations.

We note here that empirically it is found[19] that diffusion and viscosity in liquid metals are correlated; and in particular that they obey a Stokes–Einstein type relationship

$$D\eta = \text{const} \times T.$$

One would then expect to find for liquid lithium, $D^6/D^7 = \eta^7/\eta^6 = 1.08$. However, the viscosities in 99.8% pure Li^6 and 99.99% pure Li^7 have been measured, as discussed in some detail in the following section, by Ban *et al.*[16] and give the ratio 1.44 ± 0.02 already quoted above.

(*a*) *NMR measurement of self-diffusion* The relation of self-diffusion to the echo height in the pulsed NMR spin echo technique is developed by Hahn,[20] Carr and Purcell[21] and other workers[22,23] for steady magnetic gradients and infinite media.

Murday and Cotts employ the extension to pulsed gradients given by Stejskal and Tanner.[24] To their formula, essentially enabling the spin echo magnitude to be converted to an estimate of the self-diffusion coefficient, Murday and Cotts[17] point out that two additional corrections are needed before applying it to their Li measurements. The NMR technique requires penetration into the sample of radio frequency magnetic fields. Metallic Li has a skin depth of 100μ at 7 MHz, the frequency at which the experiment was carried out. The samples consisted of a powder of particles with diameter $\sim 150\mu$ or less. The Li particle diameters were of the order of the distances traversed by the atoms during a measurement of D so, as Murday and Cotts emphasize, a significant number of atoms collided with a boundary, restricting the diffusion. An extension of a theory by Neumann was used by Murday and Cotts.[25]

A powder of Li particles has significant inhomogeneous local fields due to contributions by the electron magnetic susceptibility. These fields produce large background gradients which turn out to make a significant contribution in the formula of Stejskal and Tanner relating D to the spin echo magnitude. Murday and Cotts describe a procedure for averaging the background gradient experienced by a nucleus over all nuclei, which averaging must be made to characterize the signal. We must refer the reader to their paper for this averaging.

(*b*) *Data and results* Data on the self-diffusion of Li^7 and Li^6 is collected in Table 3.1, taken from the work of Murday and Cotts.[17]

Also in Figure 3.1, graphical data is presented to display the temperature dependence of self-diffusion of Li^7 in 99.99% Li^7 and Li^6 in 99% Li^6. Nachtrieb[26] has discussed the temperature dependence of liquid metal diffusion coefficients. He found that tin, lead and indium self-diffusion

TABLE 3.1

Self-diffusion coefficients for Li^6 and Li^7 in various isotopic lithium alloys (after Murday and Cotts, 1971).

Species	Matrix	D (with corrections)	T°C
Li^7	99.99% Li^7	5.99	185
	0.01% Li^6	5.99	188
		6.11	186
		6.06	185
		7.19	225
		7.41	223
		8.58	257
Li^7 in alloy	36% Li^7	6.20	187
	64% Li^6	6.63	189
Li^7	4.4% Li^7	5.91	185
	95.6% Li^6		
Li^6 in alloy	36% Li^7	6.11	184
	64% Li^6	6.25	185
		6.63	189
Li^6	4.4% Li^7	6.62	184
	95.6% Li^6	6.92	187
		7.00	185
Li^6	0.7% Li^7	6.92	186
	99.3% Li^6	7.26	187
		7.12	186
		6.69	185
		7.14	188
		8.18	219
		8.23	224
		9.55	257

coefficients could be represented by either D versus T or $\ln D$ versus $1/T$ plots.

Murday and Cotts,[17] by assuming a linear temperature dependence

$$D = D_m + \alpha(T - T_m) \tag{3.1}$$

and making a least squares fit to the Li data find

$$D_m^7 = (5.76 \pm 0.5)\ 10^{-5}\ \text{cm}^2/\text{sec}$$

$$\alpha^7 = (0.036 \pm 0.003)\ 10^{-5}\ \text{cm}^2/\text{sec}\ ^\circ\text{C}$$

and

$$D_m^6 = (6.80 \pm 0.6)\ 10^{-5}\ \text{cm}^2/\text{sec}$$

$$\alpha^6 = (0.036 \pm 0.003)\ 10^{-5}\ \text{cm}^2/\text{sec}\ ^\circ\text{C}.$$

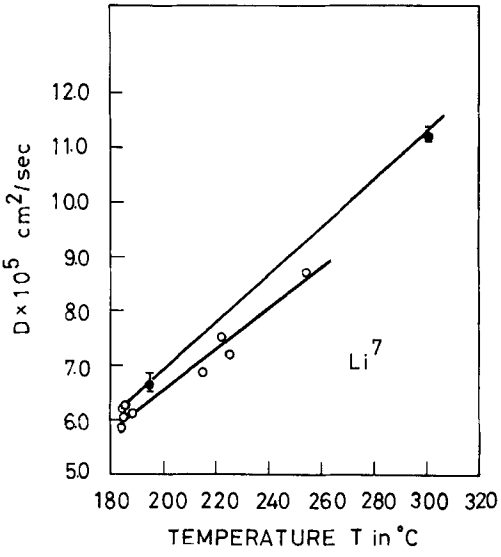

(a)

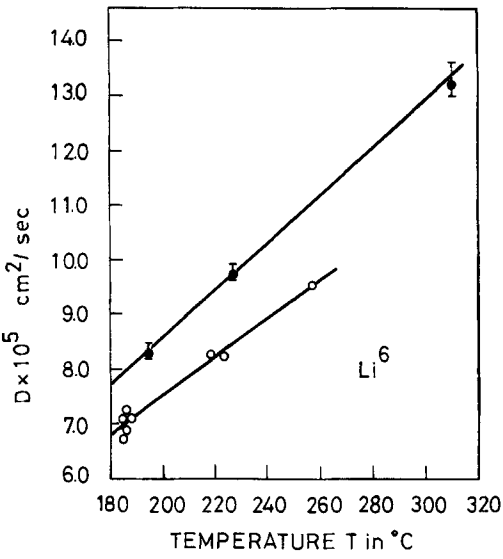

(b)

FIGURE 3.1 Self-diffusion and mutual diffusion coefficients of enriched liquid Li isotopes as function of temperature. Filled circles are for the tracer method by Löwenberg and Lodding (1967) and open circles for the NMR method by Murday and Cotts (1971).

If, on the other hand, the least squares fit is to the Arrhenius relation

$$D = D_0 \exp(-Q/RT),$$

$D_0 = (8.3 \pm 1.4)\, 10^{-4}$ cm^2/sec and $Q = 2380 \pm 160$ cal/mole for Li^7; $D_0 = (6.8 \pm 1.2)\, 10^{-4}$ cm^2/sec and $Q = 2080 \pm 160$ cal/mole for Li^6. These fits predict

$$D_m^7 = 5.8 \times 10^{-5} \text{ cm}^2/\text{sec}$$

and

$$\left(\frac{dD}{dT}\right)_{T_m}^7 = 0.034 \times 10^{-5} \text{ cm}^2/\text{sec °C}$$

while for Li^6 the values are

$$D_m^6 = 6.8 \times 10^{-5} \text{ cm}^2/\text{sec}$$

and

$$\left(\frac{dD}{dT}\right)_{T_m}^6 = 0.035 \times 10^{-5} \text{ cm}^2/\text{sec °C}.$$

Murday and Cotts point out that the ratio of the isotopic diffusion coefficients

$$D_m^6/D_m^7 = 1.18 \pm 0.07$$

is better known than either D_m^6 or D_m^7 separately, since some systematic error can be eliminated by taking the ratio.

3.2 Discussion and comparison with tracer measurements

Measurements of mutual diffusion coefficients in isotopically enriched Li have also been carried out by Löwenberg and Lodding.[27] Their data are also presented in Figure 3.1. Their results at the melting point are

$$D_{Mm}^6 = (7.8 \pm 0.2) \times 10^{-5} \text{ cm}^2/\text{sec}$$

$$D_{Mm}^7 = (5.75 \pm 0.3) \times 10^{-5} \text{ cm}^2/\text{sec}$$

where D_M^6 and D_M^7 are the mutual diffusion coefficients in the limit of isotopically pure Li^6 and Li^7 respectively. In the limit of diminishing solute concentration, the mutual diffusion coefficient approaches the self-diffusion coefficient of the solute.[28,29]

Thus, the Löwenberg and Lodding data[27] may be presented in terms of self-diffusion, since

$$\text{in matrix of } Li^7 \qquad D^7_{Mm} = D^6_m$$

and

$$\text{in matrix of } Li^6 \qquad D^6_{Mm} = D^7_m.$$

In a check on alloy concentration dependence, the self-diffusion coefficients of Li^6 and Li^7 have been measured as a function of composition using NMR, by Murday and Cotts, their results being reproduced in Figure 3.2. Their data in this figure show that the self-diffusion coefficients of Li^6 and Li^7 are relatively insensitive to the isotopic concentrations. The self-diffusion of 5% Li^7 in 95% Li^6 gives a value of

$$D_m = (5.75 \pm 0.7)\, 10^{-5}\ \text{cm}^2/\text{sec}$$

at the melting point. The Löwenberg–Lodding data[27] give the much larger value of $D_{Mm} = (7.65 \pm 0.15) \times 10^{-5}$ cm^2/sec for 7% Li in 93% Li^6. Unfavourable signal to noise ratio precluded any NMR measurement of Li^6 tracer in Li^7.

The self-diffusion data of Figure 3.2 show that there is little difference between the self-diffusion coefficients of Li^6 and Li^7 atoms in a given isotopic alloy. These data and the Löwenberg–Lodding value of D^7_{Mm} are in agreement within this percentage range. However, the D^6_{Mm} data of Löwenberg and Lodding fall well outside this percentage range.

Murday and Coots point out that there is a strong concentration dependence of self-diffusion for the solvent near both ends of the concentration range. This effect is more pronounced at the Li^7-rich end than at the Li^6-rich end of the concentration range. Examination of the data in Table 3.1 shows

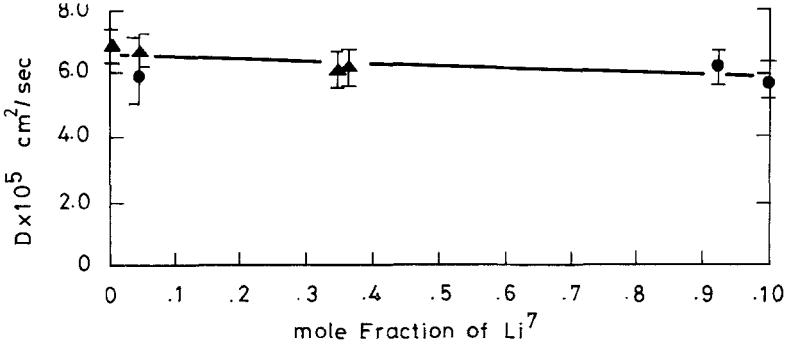

FIGURE 3.2 Self-diffusion coefficients of Li^6 and Li^7 in various isotopic Li alloys at 180.5°C. *Filled circles* are for Li^7 and filled triangles for Li^6.

that in these regions the scatter of measured values of D at a given concentration is less than the difference between mean values of D for different concentrations.

The concentration dependence is illustrated in the magnitude of the ratio (D_m^6/D_m^7) as determined from 95.6% Li^6 and 92.6% Li^7 alloys. For these alloys, $(D_m^6/D_m^7) = 1.07$ in contrast to the value of the ratio in almost isotopically pure alloys where $(D_m^6/D_m^7) = 1.18$. The fractional change in D, $[D_m^6/D_m^7 - 1]$, decreases by more than 50% for a change of just a few percent in isotope concentration.

Kruger *et al.*[18] independently made similar NMR measurements on Li^6 and Li^7. Their data, in agreement with Murday and Cotts, demonstrate a smaller isotopic mass dependence in D than was suggested by the known large isotope effect in shear viscosity,[16] to be discussed in some detail below. Murday and Cotts emphasize that their observed isotope effect is also smaller than that observed for mutual diffusion coefficients.

4 SHEAR VISCOSITY

In 1962, Ban *et al.*[16] measured the shear viscosity of the separated isotopes of molten Li. This was done by observing the viscous damping of a torsion pendulum whose bob contained a hollow spherical cavity filled with the material under test.

Their results may be summarized as follows:

i) For both Li^6 and Li^7, the viscosity varies approximately as $\exp(B/T)$ over the temperature range 180 to 300C.

ii) B has the value 458 K for Li^6 and 631 K for Li^7.

iii) The viscosity of Li^6 is 4.18 ± 0.05 millipoise (mP) at its melting temperature T_m say, of 180.4C, while that of Li^7 is 6.00 ± 0.05 mP at $T_m = 180.7$C.

iv) The ratio of the viscosity of Li^7 to that of Li^6 is 1.44 at the melting point, in contrast to the value of 1.08, the square root of the mass ratio, as predicted by simple theoretical arguments (see the discussion below).

It is relevant here to note that the separated isotopes had the compositions recorded below. The Li^6 sample contained 99.8 atomic % Li^6, 0.2% Li^7; the chemical impurities were Si 0.01%, Na 0.02% and several others; each less than 0.01%. The Li^7 sample contained 0.01% Li^6, 99.9% Li^7; the chemical impurities being Al 0.01, Sr 0.02% and several others, each less than 0.01%.

Figure 4.1, reproduced from Ban *et al.*, shows the measured viscosities of these separated isotopes as a function of temperature over the range

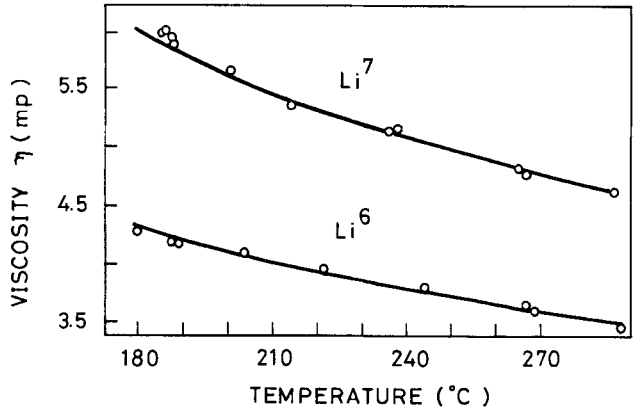

FIGURE 4.1 Viscosity of Li^6 and Li^7 as function of temperature by Ban, Randall and Montgomery (1962).

180–300C. Figure 4.2 shows the same data, but now $\log_{10} \eta$ has been plotted versus $1/T$. It can be seen that over the temperature range studied, η is well represented by the form $\exp(B/T)$ quoted in (i) above. Whereas the ratio of the viscosities at T_m is 1.44, as quoted in (iv) above, the ratio decreases gradually with increasing temperature. At the highest temperature, 278C, at which measurements were performed, the ratio has reduced to 1.32.

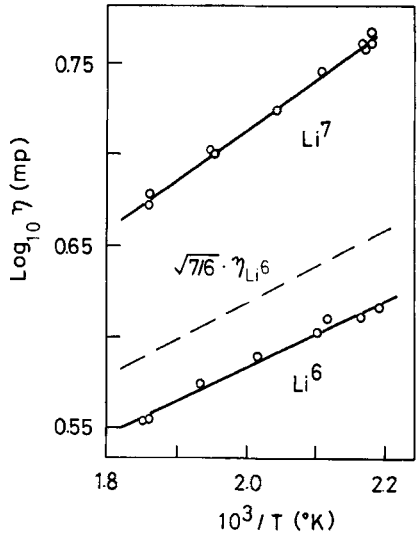

FIGURE 4.2 Plot of log η (mP) against $1/T$ for Li^6 and Li^7 by Ban, Randall and Montgomery (1962).

For naturally occurring Li, with 92.4% Li^7, 7.6% Li^6, at the melting temperature T_m = 180C, Andrade and Dobbs[30] obtain the measured value 6.02 mP. This may be compared with the (non-fundamentally based) linear interpolation between the pure isotopes of 5.86 mP quoted by Ban *et al.*[16]

It is relevant here to mention the work of Bratby and Harris,[31] who have made measurements of the shear viscosity of the liquid neon isotopes Ne^{20} and Ne^{22}. They determined the viscosity from the logarithmic decrement of an oscillating disc immersed in the liquid, using the formula of Dash and Taylor.[32] Their results are reproduced in Figure 4.3. Above 30 K, the ratio $(\eta_{22} - \eta_{20})/\eta_{20}$ is $5 \pm 1\%$. This is in agreement with the $\eta \alpha M^{1/2}$ relation given by Rowlinson[33] and by Brown and March.[34] Below this temperature, the ratio increases to $9 \pm 1\%$ at 25.4 K. They conclude that these observed departures from the classical mass scaling behaviour could arise from quantum corrections. For liquid neon, such quantum effects are expected to be observable, as discussed by Bewilogua and Gladun.[35] Bratby and Harris[31] conclude that while quantum effects seem to be the most plausible explanation of the departures observed below 30 K from the root mass scaling for the liquid neon isotopes, it is unlikely that the Li results of Ban *et al.*[16] are capable of explanation in this fashion.

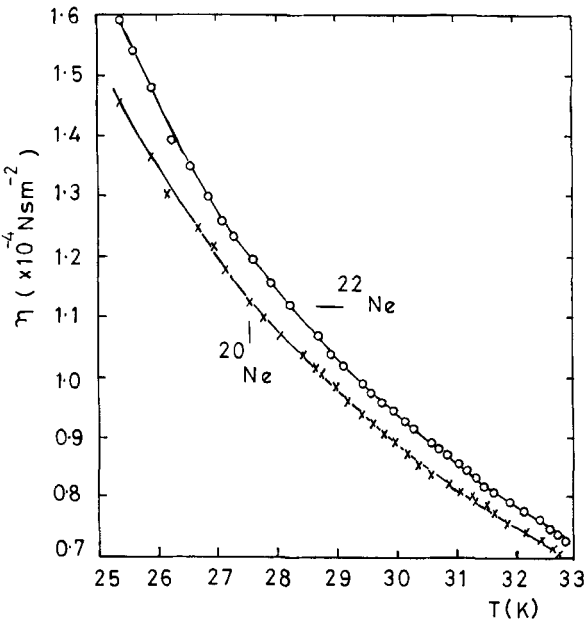

FIGURE 4.3 The shear viscosity, η, of the liquid isotopes Ne^{20} and Ne^{22} by Bratby and Harris (1972).

5 MICROSCOPIC THEORY OF HAEFFNER EFFECT

In this section we consider a liquid metal which is a mixture of two isotopes. The aim is to summarize the results of the theory of the Haeffner effect, the detail being set out in Appendix A1.

The formulation of the theory due to Parrinello *et al.*[8] leads to results which may be summarized as follows:

a) The effective valency, z_α^*, can be calculated in terms of the (concentration dependent) resistivities of isotopes 1 and 2, denoted by ρ_1 and ρ_2 respectively, from the following equation:

$$c_1 z_1^* = -c_2 z_2^* = \frac{c_1 c_2 z_1 z_2}{c_1\rho_1 + c_2\rho_2}\left(\frac{\rho_2}{z_2} - \frac{\rho_1}{z_1}\right) \tag{5.1}$$

b) The difference between ion mean-velocities is given by

$$v_1 - v_2 = BeE \times c_1 z_1^* \tag{5.2}$$

c) Ion mean-velocities must satisfy the total ion-mass flow conservation

$$c_1 M_1 v_1 + c_2 M_2 v_2 = 0 \quad \text{or} \quad v_\alpha = X_{\bar{\alpha}}(v_\alpha - v_{\bar{\alpha}})$$

where

$$X_\alpha = M_\alpha c_\alpha/(M_1 c_1 + M_2 c_2) \tag{5.3}$$

From (a), (b) and (c), we get

$$\text{if } \frac{\rho_1}{z_1} > \frac{\rho_2}{z_2},\ c_1 z_1^* < 0 \qquad \text{and then} \quad v_2 > 0,\ v_1 < 0$$

where the electric field **E** is in the positive direction of x-axis.

Typically, a current of 10^4 amps cm^{-2} is employed for 2000 hours to establish an isotopic concentration gradient in pure liquid Hg and the difference between ionic drift velocities is about 10^{-8} to 10^{-9} cm sec^{-1} required to separate the isotopes on the scale of 1 to 10 cm.[5] Therefore, in order that the theory is acceptable quantitatively, it must satisfy

$$\begin{aligned} &\text{(i)} \quad \text{If } M_1 < M_2,\ \rho_1 > \rho_2 \\ &\text{(ii)} \quad |v_1 - v_2| \sim 10^{-8\sim-9} \text{ cm sec}^{-1}. \end{aligned} \tag{5.4}$$

If the origin of the Haeffner effect is to be understood by the 'simple electron-ion interaction' defined by Eq. (A1.5), it must arise from quantum effects since $V_{e1}(k) = V_{2e}(k)$ for isotopes and the classical ionic structure factors then cancel exactly in the difference $\rho_1 - \rho_2$.

Let us calculate the quantum correction. From Eqs (A1.6) and (A1.10), we obtain

$$\rho_1 - \rho_2 = \frac{m}{ne^2} \times \frac{m}{12\pi^3\hbar^3} \int_0^{2k_f} \mathrm{d}k\, k^3 |V_{e1}(k)|^2 \{(\rho_1)_k - (\rho_2)_k\}, \quad (5.5)$$

where

$$(\rho_i)_k = \int_{-\infty}^{\infty} \mathrm{d}\omega \left[S_{ii}(k, \omega) + \sqrt{\frac{c_{\bar{i}}}{c_{\bar{i}}}} S_{ii}(k\ \omega) \right] \times \frac{\beta\hbar\omega}{e^{\beta\hbar\omega} - 1}$$

We can now use the following equations:

i) $x/(e^x - 1) = 1 - \frac{1}{2}x + \sum_{n=1}^{\infty} (-1)^{n-1} \{B_n/(2n)!\} x^{2n}$, where B_n is the Bernoulli number, namely, $B_1 = \frac{1}{6}$, $B_2 = \frac{1}{30}, \ldots$.

ii) When we define $\langle \omega^n \rangle_{ij} \equiv \int_{-\infty}^{\infty} \mathrm{d}\omega\, \omega^n S_{ij}(k, \omega)$, one can show that

$$\langle \omega^0 \rangle_{ij} = \frac{1}{\sqrt{N_i N_j}} \langle \rho_i(k) \rho_j^+(k) \rangle = S_{ij}(k),$$

$$\langle \omega^1 \rangle_{ij} = \delta_{ij} \cdot \frac{\hbar k^2}{2M_i},$$

$$\langle \omega^2 \rangle_{ij} \cong \langle \omega^2 \rangle_{ij}^{\text{classical}} = \delta_{ij} \cdot \frac{k^2}{M_i \beta}.$$

Then

$$(\rho_1)_k - (\rho_2)_k = \left\{ S_{11}(k) + \sqrt{\frac{c_2}{c_1}} S_{21}(k) - S_{22}(k) - \sqrt{\frac{c_1}{c_2}} S_{12}(k) \right\}$$
$$- \left(\frac{1}{M_1} - \frac{1}{M_2} \right) \frac{\hbar^2 k^2 \beta}{6} + 0(\hbar^4).$$

Equations (5.4), (5.5) and this equation show that the quantum correction is in the wrong direction to give the Haeffner effect.[8]

The remaining possibilities as to the origin of the Haeffner effect may be summarized as follows:

a) In the discussion above, we implicitly assume that $V_{e\alpha}(k)$ is independent of ionic mass. Otherwise, this mass-dependence might be the origin of the effect. This possibility is considered further in Section 6 below.

b) The dynamical electron-ion interaction might be the origin of the effect.

It will be useful to rewrite the expression for $\rho_1 - \rho_2$ as a sum of the two parts as follows. From Eqs (A1.6) and (A1.10)

$$\rho_1 - \rho_2 = A_m + A_q,$$

where

$$A_m = \frac{m^2}{12\pi^3\hbar^3 ne^2}\int_0^{2k_f} \mathrm{d}k\, k^3 \int_{-\infty}^{\infty} \mathrm{d}\omega \frac{\beta\hbar\omega}{e^{\beta\hbar\omega}-1} \tag{5.6}$$

$$\times [V_{e1}(k) - V_{e2}(k)][V_{e1}(k)S_{11}(k,\omega) + V_{e2}(k)S_{22}(k,\omega)]$$

$$A_q = \frac{m^2}{12\pi^3\hbar^3 ne^2}\int_0^{2k_f} \mathrm{d}k\, k^3 V_{e1}(k)V_{e2}(k) \int_{-\infty}^{\infty} \mathrm{d}\omega \frac{\beta\hbar\omega}{e^{\beta\hbar\omega}-1}\frac{S_{NC}(k,\omega)}{c_1c_2}$$

where

$$S_{NC}(k,\omega) = c_1c_2S_{11}(k,\omega) - c_1c_2S_{22}(k,\omega) + \sqrt{c_1c_2}[c_2S_{21}(k,\omega) - c_1S_{12}(k,\omega)]$$

As seen from the above expressions, A_m is the effect of the mass-dependence of the electron-ion interaction while A_q comes from the quantum correction already discussed above. A_m will be discussed in Section 6 below.

6 MODELS FOR IONIC MASS DEPENDENCE OF ELECTRON-ION INTERACTION

In this section, we shall consider three models by way of illustration of the possible ionic mass dependence of the electron-ion interaction.

6.1 Sorbello's model of moving atom with single valence electron

Before considering condensed phases, it is instructive to briefly consider, following Sorbello,[36] a moving atom with a single valence electron. In order to describe the dynamics of this valence electron, Sorbello adopted the frozen core approximation. Then the following Schrödinger equations result, in terms of the atom centre-of-mass coordinate **R** and the electron relative coordinate **r**:

$$-\frac{\hbar^2}{2(M+m)}\nabla_{\mathbf{R}}^2\frac{1}{\sqrt{V}}\exp(i\mathbf{P}\cdot\mathbf{R}/\hbar) = \frac{P^2}{2(M+m)}\frac{1}{\sqrt{V}}\exp(i\mathbf{P}\cdot\mathbf{R}/\hbar)$$

and

$$\left\{-\frac{\hbar^2}{2\mu}\nabla_{\mathbf{r}}^2 + V(r)\right\}\psi(\mathbf{r}) = \varepsilon\psi(\mathbf{r}); \frac{1}{\mu} = \frac{1}{m} + \frac{1}{M} \tag{6.1}$$

where M and m denote ionic and electronic masses respectively. Here $V(r)$ is evidently the potential energy of the electron in the field of the nucleus plus any core electrons. Since $V(r)$ may be determined by the core-electron wave functions, it will depend on the electron mass. It should be noted here that, in this model, the original electron mass m is replaced by the reduced mass μ everywhere in the expression for $V(r)$. Below, all fixed nucleus quantities (i.e. limit $M \to \infty$) are written with a tilde. For the limit $M \to \infty$ Eq. (6.1) becomes

$$\left\{-\frac{\hbar^2}{2m}\nabla_{\mathbf{r}}^2 + \tilde{V}(r)\right\}\tilde{\psi}(\mathbf{r}) = \tilde{\varepsilon}\tilde{\psi}(\mathbf{r}).$$

The main results which then emerge from Sorbello's work are:

$$V(r) = \tilde{V}\left(r\frac{\mu}{m}\right)\frac{\mu}{m} \tag{6.2}$$

or in Fourier transform:

$$V(k) = \left(\frac{m}{\mu}\right)^2 \tilde{V}\left(\frac{m}{\mu}k\right) \tag{6.3}$$

If we allow a pseudopotential which is energy dependent, i.e. $V(r) \to U(r, \varepsilon)$, then the corresponding Eqs to (6.2) and (6.3) above are:

$$U(r, \varepsilon) = \tilde{U}\left(r\frac{\mu}{m}, \varepsilon\frac{m}{\mu}\right)$$

and

$$U(k, \varepsilon) = \left(\frac{m}{\mu}\right)^2 \tilde{U}\left(\frac{m}{\mu}k; \frac{m}{\mu}\varepsilon\right).$$

These are the main predictions from Sorbello's model, in the context of the present study.

6.2 Extension of Sorbello's model to simple liquid metal

A general Hamiltonian for a simple liquid metal with two types of isotope may be written:

$$H = H_e + H_i + H_{e-i} \tag{6.4}$$

where

$$H_e = \sum_{i=1}^{N}\frac{p_i^2}{2m} + \frac{1}{2}\sum_{i\neq j}\frac{e^2}{|\mathbf{r}_i - \mathbf{r}_j|},$$

$$H_i = \sum_{\alpha=1}^{2}\sum_{i=1}^{N\alpha}\frac{P_i^{(\alpha)2}}{2M_\alpha} + \frac{1}{2}\sum_{\substack{\alpha i\\(\alpha i)\neq(\beta j)}}\sum_{\beta j} W(|\mathbf{R}_i^{(\alpha)} - \mathbf{R}_j^{(\beta)}|).$$

Here $W(r)$ is a bare ion-ion interaction, while the electron-ion interaction coupling electron (H_e) motion and ion (H_i) motion can be expressed as

$$H_{e-i} = \sum_{\alpha j} \sum_{i} V_{e\alpha}(|\mathbf{r}_i - \mathbf{R}_j^{(\alpha)}|), \tag{6.5}$$

where $V_{e\alpha}(r)$ is the interaction potential between an electron and an α type moving ion.

Based on an analogy with Eq. (6.2), it is proposed to examine a model for $V_{e\alpha}(r)$ corresponding to which is the electron-fixed ion interaction potential:

$$V_{e\alpha}(r) = a_\alpha^{-1} \tilde{V}(a_\alpha^{-1} r) \tag{6.6a}$$

or in Fourier transform,

$$V_{e\alpha}(k) = a_\alpha^2 \tilde{V}(a_\alpha k) \tag{6.6b}$$

In Eq. (6.6), a_α is a parameter to take into account the effect of ionic motion on the electron-ion interaction (cf. Eq. (6.2), where $a_\alpha = 1 + m/M_\alpha$).

Assuming, in the liquid metal phase, that

$$a_\alpha = 1 + \xi(m/M_\alpha)^\kappa$$

we have calculated the mass dependence of the Haeffner effect in Appendix A1.

We must take into account the screening effect of electrons through the dielectric function $\varepsilon(k)$, and write

$$V_\alpha^{Sc}(k) = V_{e\alpha}(k)/\varepsilon(k) = a_\alpha^2 \tilde{V}^{Sc}(a_\alpha k) \frac{\varepsilon(a_\alpha k)}{\varepsilon(k)}$$

where $\tilde{V}^{Sc}(k) = \tilde{V}(k)/\varepsilon(k)$. Then we find the result:

$$V_{e1}^{Sc}(k) - V_{e2}^{Sc}(k) = 2(a_1 - a_2)\tilde{V}^{sc}(k)\left[1 + \frac{k}{2}\left(\frac{1}{\tilde{V}^{Sc}(k)}\frac{\partial \tilde{V}^{Sc}(k)}{\partial k} + \frac{1}{\varepsilon(k)}\frac{\partial \varepsilon(k)}{\partial k}\right)\right]$$

$$+ 0(a_1 - a_2)^2$$

Then we find for the quantity A_m the result in the lowest order

$$A_m = \frac{m^2}{6\pi^3 \hbar^3 n e^2} \times (a_1 - a_2) \times (2k_f)^4 \int_0^1 \mathrm{d}k\, k^3 (\tilde{V}^{Sc}(k))^2$$

$$\times \left\{1 + \frac{k}{2}\frac{1}{\tilde{V}^{Sc}(k)}\frac{\partial \tilde{V}^{Sc}(k)}{\partial k} + \frac{k}{2}\frac{1}{\varepsilon(k)}\frac{\partial \varepsilon(k)}{\partial k}\right\}$$

$$\times \int_{-\infty}^{\infty} \mathrm{d}\omega \frac{\beta\hbar\omega}{e^{\beta\hbar\omega} - 1} \{S_{11}(k, \omega) + S_{22}(k, \omega)\}$$

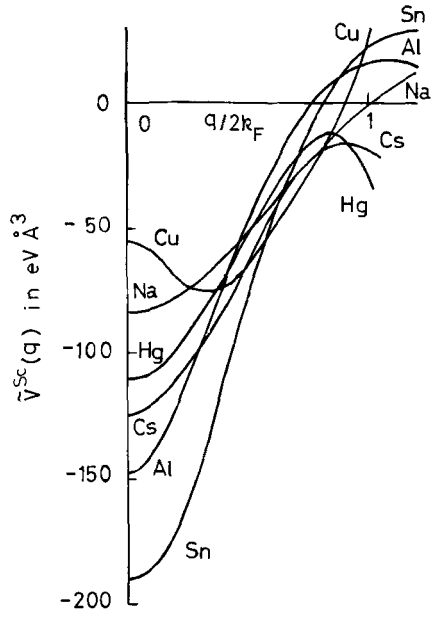

FIGURE 6.1 Screened pseudo-potentials.

We see that the sign of A_m is dependent on the details of $\tilde{V}^{Sc}(k)$ and $\varepsilon(k)$, in particular, in the range near $k = 1$. We show the behaviour of $\tilde{V}^{Sc}(k)$ for various kinds of metals and $\varepsilon(k)$ in Figures 6.1 and 6.2. We may conclude that there is the definite possibility of $A_m > 0$ in most liquid metals shown in these figures.

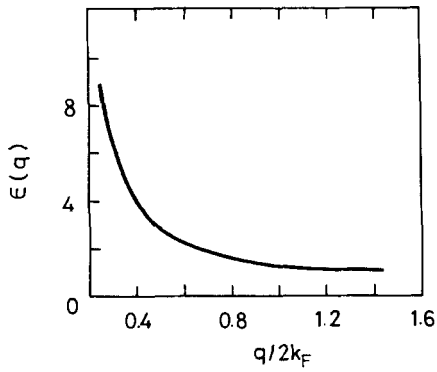

FIGURE 6.2 Lindhard dielectric constant for $r_s = 3.0$, r_s being the ratio of the radius of the spherical volume per electron to the Bohr radius.

6.3 Model of Rezayi and Suhl

Rezayi and Suhl proposed a model for a one-component solid, containing an impurity and calculated the escape rate of the impurity. In this model, the (light) impurity is characterized by its local mode, and this mode can experience instabilities which arise from non-linear, dynamical coupling between the local mode and its surroundings. Rezayi and Suhl assume that this instability means the escape of the impurity from its initial site.

Here, we shall model the effective ion dynamics in a metal by the model of Rezayi and Suhl. In particular, in Appendix A2 we calculate (a) the dynamical structure factors and (b) the electrical resistivity of the ion component. Another characteristic of the model that then emerges is that the effect of the local mode on the electrical resistivity increases anomalously as the instability is approached.

In the following section, we shall apply the model of Rezayi and Suhl to a solid Li isotopic mixture. However, by way of summary of the conclusions of the detailed treatment of Appendix A2, we conclude the present section with a brief discussion of Figure 6.3, which is related to the anomalous growth of $S(k) = \int S(k\omega)\, d\omega$ and the resistivity ρ in the model of Rezayi and Suhl.

(a) *Anomalous growth of $S(k)$ and ρ* The solutions of Mathieu's Eq. (A2.5) contain the two parameters a and q. Figure 6.3 shows the regions in the (a, q) plane where the solutions are stable or unstable. The regions are

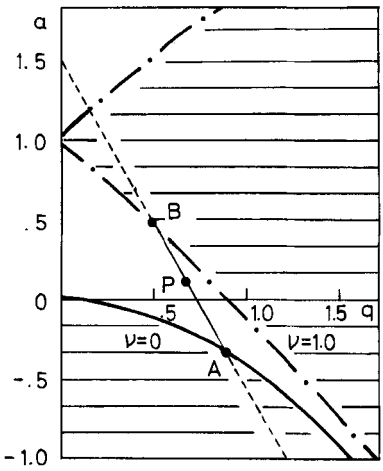

FIGURE 6.3 Characteristic exponent ν. In the first stable region bounded by $q = 0$, $\nu = 0$ and $\nu = 1$ lines, $0 < \nu < 1$.

bounded by the v-constant lines. The (a, q) corresponding to our model lies on the straight line APB as they must satisfy $a = \omega_M^2/\omega_b^2 - 2q$ due to their definitions.

The parameter q varies with respect to time t, though this variation was treated adiabatically in Mathieu's equation. Then the solution we have obtained occasionally experiences an instability as the point $P(a, q)$ approaches the points A or B.

On the other hand, the expressions (A2.7) and (A2.8) for $S(k)$ and ρ tell us that $S(k)$ and ρ increase anomalously as the point P approaches A or B.

The conditions for these instabilities can be expressed approximately as follows:

$$\text{(a)} \quad q \to \frac{\omega_M^2}{2\omega_b^2} \quad \text{or} \quad g(t) \to \frac{\omega_M^2}{3B}$$

$$\text{(b)} \quad q \to \frac{\omega_M^2}{\omega_b^2} - 1 \quad \text{or} \quad g(t) \to \frac{2}{3B}(\omega_M^2 - \omega_b^2).$$

It should be noted that these conditions are the same as those of the local mode instabilities in the work of Rezayi and Suhl. Therefore while the local mode is becoming unstable, its effect on $S(k)$ and ρ increases anomalously.

6.4 Experimental data of Dugdale *et al.* on isotopes of solid Li

Parrinello *et al.*,[8] as discussed in Section 5, have related the Haeffner effect, as already mentioned above, to the electrical resistivity of pure isotopes, say ρ_1 and ρ_2. The only directly measured resistivity data which is known to us is on solid Li, where Dugdale *et al.*[37] conclude oppositely (see, however, below). However, the tendency towards local phonon mode formation round a light isotope has implications for the interpretation. Such a model, in a form in which it might still have relevance when the long-range order is lost above the melting point, has been presented in Section 6.3 above. We now shall establish contact between Dugdale's results and the model represented in Section 6.3.

Dugdale *et al.* studied experimentally the electrical resistivity of the solid lithium and reported that the resistivity of Li^7 is larger than that of Li^6. Parrinello, Tosi and March[8] have been interested in this result as the opposite conclusion derived from the existence criterion of the Haeffner effect in their formulation of the theory for liquid lithium.

Let us discuss this problem on the basis of the result in Section 6.3. We first consider the case in which Li^6 and Li^7 systems are pure, namely, they contain no impurity. Since all phonon states in Section 6.3 are expressed

by $\phi_{\mathbf{k}}(\mathbf{x}) = (1/\sqrt{V})e^{i\mathbf{k}\cdot\mathbf{x}}$ with the eigenvalue $\omega_k \equiv Ck$, and then $\langle \mathbf{k}|\phi_{\mathbf{k}'}\rangle = \delta_{\mathbf{k},\mathbf{k}'}$ when we specify the phonon states in terms of wave vector $\mathbf{k}$ instead of $r = 1, 2, \ldots, N$, the resistivity ρ becomes

$$\rho = \frac{m^2}{12\pi^3\hbar^3 ne^2}\int_0^{2k_f} \mathrm{d}k\, k^3 |U_{ei}(k)|^2 \cdot \left\{\frac{k_B T}{M_0 C^2} F\left(\frac{\hbar Ck}{k_B T}\right)\right\} \tag{6.7}$$

where the function $F(x)$ is $x^2 e^{-x}/(1 - e^{-x})^2$.

Since $M_6 C_6^2 = M_7 C_7^2$ and $F(\hbar C_6 k/k_B T) < F(\hbar C_7 k/k_B T)$, the inequality, $\rho_7 > \rho_6$ is always satisfied. This cannot, however, explain the experiment, because Eq. (6.7) gives the difference $\rho_7 - \rho_6$ a strong temperature dependence and this is not in agreement with the experiment in which the difference in the resistivities of Li^6 and Li^7 is nearly constant as T becomes lower.

In order to seek another explanation of the experimental result, we refer to the details of lithium samples[37] used in their experiment: their resistivities are for lithium 6 (99.3% Li^6 and 0.7% Li^7) and lithium of natural isotopic composition (92.7% Li^7 and 7.3% Li^6). Note the large difference in the impurity composition! The natural lithium may have to be treated as an alloy. From Eqs (A1.8) and (A1.10), the resistivity of this alloy is

$$\begin{aligned}\rho_7^{\mathrm{tot}} &= \frac{m}{ne^2}\frac{1}{\tau} = c_1\rho_1 + c_2\rho_2 \\ &= \rho_2 + c_1[\rho_1 - \rho_2],\end{aligned} \tag{6.8}$$

where $c_1 = 0.073$, $c_2 = 0.927$, ρ_1 and ρ_2 are partial resistivities of Li^6 and Li^7 components, respectively. On the other hand, the lithium 6 sample may be treated as the pure system and then its resistivity is

$$\rho_6^{\mathrm{tot}} = \rho_6,$$

where ρ_6 is approximated by Eq. (6.7). The partial resistivity ρ_2 in Eq. (6.8) may be approximated by Eq. (6.7) as well. Now, from the discussion in the last paragraph we get

$$\begin{aligned}\rho_7^{\mathrm{tot}} - \rho_6^{\mathrm{tot}} &\cong c_1(\rho_1 - \rho_2) \\ &\cong 0.15\ \mu\Omega\ \mathrm{cm}\end{aligned} \tag{6.9}$$

It is interesting that the experimental result of Dugdale *et al.*,[37] namely $\rho_7^{\mathrm{tot}} > \rho_6^{\mathrm{tot}}$ seems to imply that

$$\rho_1 > \rho_2 \tag{6.10}$$

in terms of the partial resistivity ρ_1 and ρ_2 of natural lithium. This inequality is just the same as that of the existence criterion of the Haeffner effect in the

formulation by Parrinello, Tosi and March.[8] It may be interesting that with the use of Eqs (6.9) and (5.1) we estimate the magnitude of the effective valences of Li^6 and Li^7 in the natural solid lithium. From $c_1 = 0.073$, $c_2 = 0.927$ and $c_1\rho_1 + c_2\rho_2 \equiv \rho_7^{tot}$, we get from the data by Dugdale *et al.*[37]

$$\underset{(80°K)}{2.1} \gtrsim \frac{\rho_1 - \rho_2}{c_1\rho_1 + c_2\rho_2} \gtrsim \underset{(320°K)}{0.2}$$

$$\underset{(80°K)}{-1.9} \lesssim z_1^* \lesssim \underset{(320°K)}{-0.2},$$

$$\underset{(80°K)}{0.2} \gtrsim z_2^* \gtrsim \underset{(320°K)}{0.0}$$

It is possible to interpret Eq. (6.10) on the basis of the model of Section 6.3. Li^6 (Li^7) in the natural lithium may be modelled by the local phonon modes (the Debye phonon modes or the band phonon modes). As discussed in Section 6.3, the effect of the local modes (unlike the other kind of modes) to the electrical resistivity can, under some circumstances, increase anomalously. This may explain Eq. (6.10).

From Eqs (A1.4) and (A1.10) we find in the notation of Appendix A1

$$\frac{|\mathbf{f}_2|}{|\mathbf{f}_1|} = \frac{\rho_2}{\rho_1}$$

This suggests that the anomalous growth in the resistivity may be accompanied by the anomalous growth of the electron drag force felt by the Li^6 in the local modes, according to Newton's Third Law. Li^6 then would be forced to move towards the anode. On the other hand, vacancies are left behind in this process of migration. Though the effective force acting on Li^7 is relatively weak, it would force Li^7 to move towards the cathode with the help of the vacancy mechanism in such a way that the migrations of Li^6 and Li^7 satisfy the total mass flow conservation law, Eq. (A1.13).

The discussion above may also be relevant in natural liquid lithium though, of course, the language of vacancies has to be modified, perhaps along lines proposed by Eyring.

7 DISCUSSION AND SUMMARY

That a lot remains to be done quantitatively on isotope effects in liquid metals is quite clear. While some of the ideas by which mass effects resembling those observed are by now laid down, it is still true that nowhere is the theory to date in better than semiquantitative agreement with experiment.

It remains to study, in more detail, the effects of indirect dynamic ion–ion interactions. A start on this area has been made by McCaskill and March[38] and by March and Suhl[39] but clearly this is worth further exploration.

More measurements on light isotopes of liquid metals would be highly desirable; e.g. Be isotopes, but the toxicity of this material no doubt constitutes a major obstacle to progress.

The question of local modes round a light impurity, well treated in a crystalline solid, when the long-range order of the host material is lost is plainly an area on which further work, both experimental and theoretical, should be of value.

Acknowledgment

One of us (N.H.M.) wishes to acknowledge many valuable discussions on the area embraced in this article with Dr J. S. McCaskill, and the other (M.G.) would like to express his sincere thanks to the Japanese Ministry of Education for the Grant supporting his study leave abroad in 1984.

References

1. E. Haeffner, *Nature*, **172**, 775 (1953).
2. H. B. Huntington in *American Society for Metals*, Metals Park, Ohio 1973, p. 155.
3. E. H. Rezayi and H. Suhl, *Phys. Rev. Lett.*, **45**, 1115 (1980); *Phys. Rev.*,**B25**, 2324 (1982).
4. S. G. Epstein, *Liquid metals: Chemistry and Physics:* Ed. S. Beer, (Dekker: New York).
5. T. E. Faber, *An introduction to the theory of liquid metals* (Cambridge: University Press) 1972.
6. R. Landauer and J. W. F. Woo, *Phys. Rev.*, **B10**, 1266 (1974).
7. D. Stroud, *Phys. Rev.*, **B13**, 4221 (1976).
8. M. Parrinello, M. P. Tosi and N. H. March, Lett. *Nuovo Cimento*, **12**, 605 (1975).
9. K. E. Grew, *Transport of Fluids*: Ed. H. J. M. Hanley (Dekker: New York) 1969.
10. O. D. Gonzalez and R. A. Oriani, *Trans. Metall. Soc. A.I.M.E.*, **233**, 1878 (1965).
11. M. Gerl, *Zeits für Naturforschung*, **26A**, 1 (1971).
12. A. Ott and A. Lunden, *Zeits für Naturforschung*. **19A**, 822 (1964).
13. J. D. Verhoeven, *Metall. Rev.*, **8**, 311 (1963); *Phys. Fluids*, **12**, 1783 (1969).
14. D. A. Rigney in *Liquid metals* (Inst Phys Conf. Series No. **30**) Bristol, 1977, p. 619.
15. B. N. Bhat and R. A. Swalin, *Acta Metall.*, **20**, 1387 (1972).
16. N. T. Ban, C. M. Randall and D. J. Montgomery, *Phys. Rev.*, **128**, 6 (1962).
17. J. S. Murday and R. M. Cotts, *Zeits für Naturforschung*, **26a**, 85 (1971).
18. G. J. Krüger, W. Müller-Warmuth and A. Klemm, *Zeits für Naturforschung*, **26a**, 94 (1971).
19. See, for example, H. J. Saxton and O. D. Sherby, *Trans. Am. Soc. Metals*, **55**, 826 (1962).
20. E. L. Hahn, *Phys. Rev.*, **80**, 580 (1950).
21. H. Y. Carr and E. M. Purcell, *Phys. Rev.*, **94**, 630 (1954).
22. A. Abragam, *Principles of nuclear magnetism* (Oxford: University Press) 1961.
23. H. C. Torrey, *Phys. Rev.*, **104**, 563 (1956).
24. E. O. Stejskal and J. E. Tanner, *J. Chem. Phys.*, **42**, 288 (1965).
25. See J. S. Murday and R. M. Cotts, *J. Chem. Phys.*, **48**, 4938 (1968).
26. N. H. Nachtrieb, *Advances Phys.*, **16**, 309 (1967).
27. L. Löwenberg and A. Lodding, *Zeits für Naturforschung*, **22a**, 2077 (1967).
28. R. J. Bearman, *J. Phys. Chem.*, **65**, 1961 (1961).

29. D. W. McCall and D. C. Douglass, *J. Phys. Chem.*, **69**, 2001 (1965).
30. E. N. da C. Andrade and E. R. Dobbs, *Proc. Roy. Soc.*, **A211**, 12 (1952).
31. P. Bratby and E. A. Harris, *Phys. Letts.*, **40A**, 25 (1972).
32. J. G. Dash and R. D. Taylor, *Phys. Rev.*, **105**, 7 (1957); 106, 3 (1957).
33. J. S. Rowlinson, *Physica*, **19**, 303 (1953).
34. R. C. Brown and N. H. March, *Phys. Chem. Liquids*, **1**, 141 (1968).
35. L. Bewilogua and C. Gladun, *Cont. Phys.*, **9**, 277 (1968).
36. R. S. Sorbello, *Phys. Rev.*, **A30**, 683 (1984).
37. J. S. Dugdale, D. Gugan and K. Okumura, *Proc. Roy. Soc.*, **A263**, 407 (1961).
38. J. S. McCaskill and N. H. March, *Surface Science*, **131**, 34 (1983); see also *Int. J. Quantum Chem.*, **14S**, 681 (1980).
39. N. H. March and H. Suhl, *Phys. Chem. Liquids*, **14**, 159 (1984).
40. J. S. Rousseau, J. C. Stoddart and N. H. March, *J. Phys. C 5*, L175 (1972).
41. See, for example, the review by M. Huberman and G. V. Chester, *Advances Physics*, **24**, 489 (1975), and other references given there.
42. See also J. S. McCaskill and N. H. March, *J. Phys. Chem. Solids*, **45**, 215 (1984).

Appendix A1 Relation of Haeffner effect to the electrical resistivity of liquid metals

An external, static electric field $\mathbf{E} = (E, 0, 0)$ is applied to the liquid metal in the positive direction of the x-axis and a steady current of electrons is established. The system may be described by the Hamiltonian:

$$\begin{aligned} \mathscr{H} &= \mathscr{H}_0 + H_{ei} \\ \mathscr{H}_0 &= \mathscr{H}_e + \mathscr{H}_i, \end{aligned} \tag{A1.1}$$

where $\mathscr{H}_i$ is the effective Hamiltonian of the two kinds of ion-components, and $\mathscr{H}_e$ is the effective Hamiltonian of the electron component. The most general expression of H_{ei} may be written

$$\begin{aligned} H_{ei} = \frac{1}{V} \sum_{\mathbf{k}} \int \mathrm{d}\omega \sum_{\mathbf{p}\sigma} \sum_{\mathbf{p}'} \delta_{\mathbf{p}-\mathbf{p}',\hbar\mathbf{k}} \delta(\{\varepsilon_p - \varepsilon_{p'}\}/\hbar - \omega) \\ \times \sum_{\alpha=1,2} \langle \mathbf{p}' | U_{e\alpha}(\mathbf{k}, \omega) | \mathbf{p} \rangle \rho_\alpha^+(\mathbf{k}) a_{\mathbf{p}'\sigma}^+ a_{\mathbf{p}\sigma} \end{aligned}$$

where $a_{\mathbf{p}\sigma}^+$ and $a_{\mathbf{p}\sigma}$ are creation and annihilation operators of a $\mathbf{p}\sigma$-electron respectively:

$$\rho_\alpha(\mathbf{k}) = \sum_{i=1}^{N\alpha} \exp(-i\mathbf{k} \cdot \mathbf{R}_i^{(\alpha)}),$$

$\mathbf{R}_i^{(\alpha)}$ being the position vector of the ith ion of the α-ion component. $\langle \mathbf{p}' | U_{e\alpha}(\mathbf{k}, \omega) | \mathbf{p} \rangle$ denotes the interaction matrix element corresponding to

the electron-α type ion interaction. The remaining factors mean energy-momentum conservation in the process of interaction. We may assume that $\mathscr{H}_e$ describes the assembly of effectively free electrons and then

$$\frac{\mathrm{Tr}[e^{-\beta\mathscr{H}_e}a^+_{\mathbf{p}\sigma}a_{\mathbf{p}\sigma}]}{\mathrm{Tr}[e^{-\beta\mathscr{H}_e}]} = \{\exp[\beta(\varepsilon_{\mathbf{p}+\tau e\mathbf{E}} - \mu)] + 1\}^{-1} \equiv f(\mathbf{p} + \tau e\mathbf{E})$$

where $\beta = 1/k_B T$, $\varepsilon_p = p^2/2m$, τ is the electronic relaxation time and μ is the chemical potential.

The 'electron-wind' force, $\mathbf{f}_\alpha$, acting on the α-ion component may be calculated as the average of the force operator $\sum_{j=1}^{N_\alpha}[-\nabla^{(\alpha)}_{\mathbf{R}_j}H_{ei}]/N_\alpha$. The method has similarities to that of Rousseau *et al.*[40,41,42] In the case of weak electron-ion interaction, however, we can get the same expression for $\mathbf{f}_\alpha$ directly from the work of Baym. In Born approximation for the treatment of electron inelastic scattering, the rate at which momentum $\hbar\mathbf{k}$ transfers from the electrons to the α-ion component is

$$\begin{aligned} W_\alpha(\mathbf{k}) = \frac{2\pi}{V^2\hbar^2}\int \mathrm{d}\omega \sum_{\mathbf{p},\mathbf{p}'}\delta_{\mathbf{p}-\mathbf{p}',\hbar\mathbf{k}}\delta(\{\varepsilon_p - \varepsilon_{p'}\}/\hbar - \omega) \\ \times \sum_\beta \langle\mathbf{p}'|U_{e\alpha}(\mathbf{k},\omega)|\mathbf{p}\rangle\langle\mathbf{p}|U_{e\beta}(-\mathbf{k},-\omega)|\mathbf{p}'\rangle\{N_\beta/N_\alpha\}^{1/2}S_{\beta\alpha}(\mathbf{k},\omega) \\ \times [f(\mathbf{p}+\tau e\mathbf{E})(1-f(\mathbf{p}'+\tau e\mathbf{E}) \\ - \exp(-\beta\hbar\omega)f(\mathbf{p}'+\tau e\mathbf{E})(1-f(\mathbf{p}+\tau e\mathbf{E}))] \end{aligned} \tag{A1.2}$$

where

$$S_{\beta\alpha}(\mathbf{k},\omega) = \int \frac{\mathrm{d}t}{2\pi}\exp(i\omega t)\langle\rho_\beta(\mathbf{k},t)\rho^+_\alpha(\mathbf{k})\rangle/\{N_\beta N_\alpha\}^{1/2},$$

$\rho(\mathbf{k},t)$ and $\langle\cdots\rangle$ meaning the Heisenberg representation and ensemble average with respect to $\mathscr{H}_i$, respectively. The expression for $\mathbf{f}_\alpha$ is then given by

$$\mathbf{f}_\alpha = \sum_{\mathbf{k}}\hbar\mathbf{k}W_\alpha(\mathbf{k}). \tag{A1.3}$$

In the case of a weak electric field, the force $\mathbf{f}_\alpha$ is proportional to $\tau e\mathbf{E}$. Let us define a quantity τ_α by

$$\mathbf{f}_\alpha = \frac{-\tau}{\tau_\alpha}z_\alpha e\mathbf{E}. \tag{A1.4}$$

From Eqs (A1.2), (A1.3) and (A1.4)

$$\begin{aligned} \frac{1}{\tau_\alpha} = \frac{\pi\beta}{mz_\alpha V^2}\sum_{\mathbf{k}}k_x^2\sum_{\substack{p\alpha\\ \mathbf{p}'}}\int \mathrm{d}\omega\delta_{\mathbf{p}-\mathbf{p}',\hbar\mathbf{k}}\delta([\varepsilon_p - \varepsilon_{p'}]/\hbar - \omega)f(\mathbf{p})(1-f(\mathbf{p}')) \\ \times \sum_{\beta=1,2}\langle\mathbf{p}'|U_{e\alpha}(\mathbf{k},\omega)|\mathbf{p}\rangle\langle\mathbf{p}'|U_{e\beta}(\mathbf{k},\omega)|\mathbf{p}\rangle^*\sqrt{\frac{c_\beta}{c_\alpha}}S_{\beta\alpha}(\mathbf{k},\omega). \end{aligned}$$

In the case of the 'simple interaction,' namely

$$\langle \mathbf{p}' | U_{e\alpha}(\mathbf{k}, \omega) | \mathbf{p} \rangle \equiv V_{e\alpha}(k), \tag{A1.5}$$

one finds

$$\frac{1}{\tau_\alpha} = \frac{m}{12\pi^3 h^3 z_\alpha} \int_0^{2k_f} \mathrm{d}k\, k^3 \sum_{\beta=1,2} V_{e\beta}^*(k) V_{e\alpha}(k) \sqrt{\frac{c_\beta}{c_\alpha}} \int_{-\infty}^{\infty} \frac{S_{\beta\alpha}(\mathbf{k}, \omega)\beta\hbar\omega}{\exp(\beta\hbar\omega - 1}\, \mathrm{d}\omega. \tag{A1.6}$$

In the limit of the one-component ion liquid, this expression reduces to that for the relaxation time given in the work of Baym.

The total force acting on the α-type ion is the sum of the direct term $z_\alpha e\mathbf{E}$ and the 'electron drag' term $\mathbf{f}_\alpha$. The resultant force is conveniently expressed as $z_\alpha^* e\mathbf{E}$, z_α^* being termed an 'effective valency':

$$z_\alpha^* = z_\alpha \left(1 - \frac{\tau}{\tau_\alpha}\right). \tag{A1.7}$$

Now the force-balance equation in the electron component is

$$-Ne\underset{\sim}{\mathbf{E}} - \sum_\alpha N_\alpha \mathbf{f}_\alpha = 0 \qquad \left(N \equiv \sum_\alpha z_\alpha N_\alpha\right),$$

and by making use of Eq. (A1.4) we find

$$\tau = \bar{z} \Big/ \sum_\beta c_\beta \frac{z_\beta}{\tau_\beta}, \qquad \left(\bar{z} \equiv \sum_\alpha c_\alpha z_\alpha\right). \tag{A1.8}$$

In fact, the unknown quantity τ can be taken to be defined by this equation. From Eqs (A1.7) and (A1.8) we obtain

$$\begin{aligned} z_\alpha^* &= z_\alpha \left(1 - \frac{\bar{z}}{\tau_\alpha} \Big/ \left(\sum_\beta \frac{z_\beta}{\tau_\beta} c_\beta\right)\right) \\ &= z_\alpha - \bar{z}\rho_\alpha \Big/ \sum_\beta c_\beta \rho_\beta, \end{aligned} \tag{A1.9}$$

where a 'partial electrical resistivity' ρ_α is defined by

$$\rho_\alpha \equiv \frac{m}{ne^2} \frac{z_\alpha}{\tau_\alpha}. \tag{A1.10}$$

It should be noted that

$$\sum_\alpha c_\alpha z_\alpha^* = 0, \tag{A1.11}$$

which is another expression of the force balance equation in the electron component. From Eqs (A1.9) and (A1.11) we get Eq. (5.1).

The responses of the ion-components in the system under consideration defined by Eq. (A1.1) may be approximately treated in such a way that this system has applied to it a 'fictitious' external electric field $z_\alpha^* e\mathbf{E}$. Let us then consider a system defined by the following Hamiltonian:

$$H_i^{\text{eff}} = H_i + H' \tag{A1.12}$$

where $H_i \equiv [\mathscr{H}_i]_{\mathbf{E}=0}$ and

$$H' = -\sum_{\beta=1,2} N_\beta z_\beta^* eEx_\beta,$$

E and x_β being, respectively, the x-component of $\mathbf{E}$ and $\sum_{j=1}^{N_\beta} \mathbf{R}_j^{(\beta)}/N_\beta$. There exist the following force-balance equations:

$$-\sum_\beta \sum_{j=1}^{N_\beta} \nabla_{\mathbf{R}_j^{(\beta)}} H_i = 0 \qquad \text{(internal force balance)}$$

$$-\sum_\beta \sum_{j=1}^{N_\beta} \nabla_{\mathbf{R}_j^{(\beta)}} H' = (N_1 + N_2) \sum_\beta c_\beta z_\beta^* e\mathbf{E}$$

$$= 0 \qquad \text{(external force balance Eq.) (A1.11)).}$$

We now introduce a mean ion-velocity v_α as

$$v_\alpha = \text{Tr}\ \hat{w}_i \dot{x}_\alpha$$

where $\hat{w}_i$ is the statistical density matrix corresponding to Eq. (A1.12) and $\dot{x}_\alpha \equiv \mathrm{d}x_\alpha/\mathrm{d}t$. From the above force balance equations and the theorem of Ehrenfest, we obtain the total mass-flow conservation law (= total momentum conservation law) as

$$\sum_\beta c_\beta M_\beta v_\beta = 0. \tag{A1.13}$$

This is Eq. (5.3).

Now we may assume that H' is sufficiently weak and is introduced adiabatically in the remote past. By linear response theory we can obtain straightforwardly

$$v_\alpha = \sum_{\beta=1,2} \frac{z_\beta^* eE}{n_\alpha} \lim_{\omega\to 0} \lim_{k_x\to 0} \frac{i\omega}{k_x^2} \tilde{\chi}_{\alpha\beta}(|k_x|, \omega), \tag{A1.14}$$

where

$$\tilde{\chi}_{\alpha\beta}(k, \omega) = \int_0^\infty \mathrm{d}t \exp(i\omega t) \frac{1}{i\hbar V} \frac{1}{\text{Tr}\ e^{-\beta H_i}} \text{Tr}\ e^{-\beta H_i}[\rho_\alpha(\mathbf{k}, t), \rho_\beta^+(\mathbf{k})].$$

From Eqs (A1.13), (A1.14) and

$$\text{Im}\,\tilde{\chi}_{\alpha\beta}(k,\omega) = -(\pi/\hbar)[1 - \exp(-\beta\hbar\omega)](n_\alpha n_\beta)^{1/2}[S_{\alpha\beta}(k,\omega)]_{E=0},$$

$$v_1 - v_2 = Bc_1 z_1^* eE$$

where

$$B = \frac{\pi\beta}{(c_1c_2)^2} \lim_{\omega\to 0} \lim_{k_x\to 0} \frac{\omega^2}{k_x^2} S_{cc}(|k_x|,\omega)$$

while

$$S_{cc}(k,\omega) = c_1c_2\{c_2S_{11}(\mathbf{k},\omega) + c_1S_{22}(\mathbf{k},\omega) - 2(c_1c_2)^{1/2}S_{12}(\mathbf{k},\omega)\}_{E=0}.$$

Then we get Eq. (5.2).

Appendix A2 Dynamical structure factor and resistivity for the model of Rezayi and Suhl

We consider a system consisting of $N-1$ host atoms with atomic mass M_0 and an impurity located at the origin. The dynamics of the system may be described by $\mathbf{\Phi}(\mathbf{x}, t)$ which is a displacement vector of the atom having its equilibrium position at $\mathbf{x}$. Rezayi and Suhl gave the model Lagrangian governing the motion of $\mathbf{\Phi}$ in the continuum limit. This model is characterized by the coupling of the impurity with its nearest neighbours with a harmonic force (coupling constant ε) plus an anharmonic term (coupling constant b). Let us denote the orthogonal complete set of frequency eigenfunctions of the harmonic field ($b = 0$) of this model by

$$\mathbf{\Phi}_{rl}(\mathbf{x}, t) = \mathbf{e}_l \phi_r(\mathbf{x}) \exp(i\omega_r t),\ l = 1, 2, 3 \quad \text{and} \quad r = 1, 2, \ldots, N,$$

where ω_r is the eigenfrequency and $\mathbf{e}_l$ the unit vector of the l-coordinate axis. The eigenfunctions ϕ_r can be classified into two groups: the impurity-disturbed states ($r = 1, 2, \ldots, M$) and the impurity-unperturbed states ($r = M+1, \ldots, N$). In the case when $\varepsilon > 0$ the former consists of the impurity-perturbed band-states ($r = 1, 2, \ldots, M-1$) and the localized state ($r = M$) localized around the impurity. In what follows we will treat only this case.

Let us define the canonical dynamical variable set (q_{rl}, p_{rl}) by

$$q_{rl}(t) = \mathbf{e}_l \rho^{1/2} \int \mathrm{d}\mathbf{x}\, \phi_r^*(\mathbf{x})\mathbf{\Phi}(\mathbf{x}, t)$$

$$p_{rl}(t) = \frac{\mathbf{e}_l}{\rho^{1/2}} \int d\mathbf{x}\, \phi_r(\mathbf{x})\boldsymbol{\pi}(\mathbf{x}, t)$$

where ρ is the mass density and $\pi(\mathbf{x}, t)$ the canonical momentum conjugate to $\Phi(\mathbf{x}, t)$. The Hamiltonian of Rezayi and Suhl is given by

$$H = \sum_{rl} \frac{1}{2} (p^*_{rl} p_{rl} + \omega_r^2 q^*_{rl} q_{rl}) - \frac{B}{4} \left[\sum_{l=1}^{3} \left(\sum_{r \leq M} q_{rl} \right)^2 \right]^2 \tag{A2.1}$$

where $B = b/\rho\varepsilon$.[4]

One now defines the function

$$f_{rl,r'l'}(t) = \frac{i}{\hbar} \langle [q_{rl}(t), q^*_{r'l'}] \rangle,$$

$q_{rl}(t)$ being the Heisenberg representation of q_{rl}, and if this quantity can be calculated then one can obtain the dynamical structure factor, $S(k, \omega)$, from the relation

$$S_{rl,r'l'}(\omega) = \frac{1}{1 - \exp(-\hbar\omega\beta)} \frac{\hbar}{i} \int_{-\infty}^{\infty} \frac{\mathrm{d}t}{2\pi} \exp(i\omega t) f_{rl,r'l'}(t) \tag{A2.2}$$

$$S(k, \omega) = \frac{1}{N} |\langle \rho(\mathbf{k}) \rangle|^2 \delta(\omega) + \frac{1}{M_0} \sum_{rl} \sum_{r'l'} (\mathbf{k}e_l)(\mathbf{k}e_{l'}) \langle \mathbf{k} | \phi_r \rangle \langle \phi_{r'} | \mathbf{k} \rangle S_{rlr'l'}(\omega) \tag{A2.3}$$

From the Hamiltonian (A2.1) and the Heisenberg equation of motion one finds

$$\frac{\mathrm{d}^2}{\mathrm{d}t^2} f_{r'l'}(t) + \omega_r^2 f_{rl,r'l'}(t) = \theta(M - r) B \frac{i}{\hbar} \left\langle \left[\sum_{r_1 \leq M} q_{r_1 l}(t) \sum_{l_2} \left(\sum_{r_2 \leq M} q_{r_2 l_2}(t) \right)^2, q^*_{r'l'} \right] \right\rangle$$

with the initial conditions

$$[f_{rl,r'l'}(t)]_{t=0} = 0, \qquad \left[\frac{\mathrm{d}}{\mathrm{d}t} f_{rl,r'l'}(t) \right]_{t=0} = \delta_{rr'} \delta_{ll'},$$

where $\theta(r) = 1$ for $r \geq 0$ and $\theta(r) = 0$ for $r < 0$.

For $r > M$, the effect of the anharmonic coupling vanishes. For $r \leq M$, the anharmonic term in the equation of motion is treated by an approximation equivalent to that of Rezayi and Suhl:

i) For $r \leq M - 1$, we neglect the anharmonic term.

ii) For $r = M$

$$\sum_{r_1 \leq M} q_{r_1 l}(t) \sum_{l_2} \left(\sum_{r_2 \leq M} q_{r_2 l_2}(t) \right)^2 \doteqdot 3 \left(\sum_{r \leq M-1} q_{rl}(t) \right)^2 q_{Ml}(t) \doteqdot 3[g(t) + g(t) \cos 2\omega_b t] q_{Ml}(t)$$

where $\omega_b = 0.84\,\omega_D$ (Debye frequency) and $g(t)$ is the slowly time-varying part of $(\sum_{r\le m-1} q_{rl}(t))^2$, which is treated as constant in the equation of motion. Then one obtains

$$f_{rl,r'l'}(t) = \delta_{ll'}\delta_{rr'}\frac{1}{\omega_r}\sin\omega_r t \quad \text{for} \quad r \neq M : \delta_{ll'}\delta_{rr'} f(t) \quad \text{for} \quad r = M \tag{A2.4}$$

and under the transformation

$$x = \omega_b t, \quad y(x) = \omega_b f(t), \quad a = \frac{\omega_M^2 - 3Bg}{\omega_b^2}, \quad q = \frac{3Bg}{2\omega_b^2}$$

$$\frac{d^2y(x)}{dx^2} + (a - 2q\cos 2x)y(x) = 0 \qquad \text{(Mathieu's equation)} \tag{A2.5}$$

with initial conditions

$$y(0) = 0 \quad \text{and} \quad \left.\frac{dy}{dx}\right|_{x=0} = 1.$$

Hence

$$f(t) = \omega_b^{-1} se_\nu(\omega_b t)/se'_\nu(0),$$

where $se'_\nu(0) = d/dx\, se_\nu(x)|_{x=0}$, and the characteristic exponent ν is determined by

$$ce_\nu(\pi) = ce_\nu(0)\cos\pi\nu.$$

The functions $se_\nu(x)$ and $ce_\nu(x)$ are defined by

$$ce_\nu(x) = [F_\nu(x) + F_\nu(-x)]/2$$

and

$$se_\nu(x) = [F_\nu(x) - F_\nu(-x)]/2i$$

$F_\nu(x)$ being the Bloch-type solution of the equation of Mathieu. For small q corresponding to the physical situation we want to consider

$$f(t) = \frac{1}{\omega_b \nu}\left[\sin(\omega_b \nu t) + q\left\{\frac{1}{4(\nu-1)}\sin((\nu-2)\omega_b t) - \frac{1}{4(\nu+1)}\sin(\nu+2)\omega_b t)\right\} + \cdots\right] \tag{A2.6}$$

Equations (A2.2)–(A2.6) lead to the dynamical structure factor $S(k, \omega)$ as $1/N|\langle\rho(\mathbf{k})\rangle|^2\,\delta(\omega) + \sum_{r=1}^{N} S_r(k, \omega)$, where

$$S_r(k, \omega) = \frac{k^2}{M_0}|\langle\mathbf{k}|\phi_r\rangle|^2 \frac{\hbar}{1 - e^{-\hbar\omega\beta}} \frac{1}{2\omega_r}[\delta(\omega - \omega_r) - \delta(\omega + \omega_r)]$$

for $r \neq M$

$$S_M(k, \omega) = \frac{k^2}{M_0}|\langle\mathbf{k}|\phi_M\rangle|^2 \frac{\hbar}{1 - e^{-\hbar\omega\beta}} \frac{1}{2\omega_b v}\left\{[\delta(\omega - \omega_b v) - \delta(\omega + \omega_b v)]\right.$$

$$+ \frac{q}{4(v-1)}[\delta(\omega - \omega_b(v-2)) - \delta(\omega + \omega_b(v-2))]$$

$$\left. - \frac{q}{4(v+1)}[\delta(\omega - \omega_b(v+2)) - \delta(\omega + \omega_b(v+2))]\right\}$$

and from this result it follows that the static structure factor $S(k)$ is given by

$$S(k) = \int_{-\infty}^{\infty} d\omega\, S(k, \omega) = \frac{1}{N}|\langle\rho(\mathbf{k})\rangle|^2 + \sum_{r=1}^{N} S_r(k) \qquad \text{(A2.7)}$$

where

$$S_r(k) = \frac{k^2}{M_0}|\langle\mathbf{k}|\phi_r\rangle|^2 \frac{\hbar}{2\omega_r}\coth(\hbar\omega_r\beta/2) \quad \text{for} \quad r \neq M$$

and

$$S_M(k) = \frac{k^2}{M_0}|\langle\mathbf{k}|\phi_M\rangle|^2 \frac{\hbar}{2\omega_b v}$$

$$\times\left\{\coth(\hbar\omega_b v\beta/2) + \frac{q}{4(v-1)}\coth(\hbar\omega_b(v-2)\beta/2) - \frac{q}{4(v+1)}\right.$$

$$\left.\times\coth(\hbar\omega_b(v+2)\beta/2\right\}$$

Finally, following the approach of Baym, we can calculate the electronic resistivity associated with the present model as

$$\rho = \frac{m^2}{12\pi^3 ne^2}\cdot\int_0^{2_f} dk\, k^3|U_{ei}(k)|^2\cdot\int_{-\infty}^{\infty}\frac{d\omega}{2\pi}\cdot\frac{\hbar\beta\omega}{e^{\hbar\omega\beta} - 1}S(k, \omega)$$

$$\rho = \sum_{r=1}^{N}\rho_r,\ \rho_r \equiv \frac{m^2\beta}{12\pi^3\hbar ne^2}\int_0^{2k_f} dk\, k^3|U_{ei}(k)|^2\cdot\frac{k^2}{M_0}|\langle\mathbf{k}|\phi_r\rangle|^2\cdot f_r(k)$$

(A2.8)

where U_{ei} is the interaction between electron and ion,

$$f_r(k) = \frac{1}{(e^{\hbar\omega_r\beta} - 1)(1 - e^{-\hbar\omega_r\beta})} \qquad \text{for} \quad r \neq M,$$

$$f_M(k) = \frac{1}{(e^{\hbar\omega_b v\beta} - 1)(1 - e^{-\hbar\omega_b v\beta})} + \frac{q}{4(v-1)} \frac{v-2}{(e^{\hbar\omega_b(v+2)\beta} - 1)(1 - e^{-\hbar\omega_b(v-2)\beta})} - \frac{q}{4(v+1)} \frac{v+2}{(e^{\hbar\omega_b(v+2)\beta} - 1)(1 - e^{-\hbar\omega_b(v+2)\beta})}.$$

These results, for $S(k, \omega)$ and ρ, are consequences of course of the simple model of Rezayi and Suhl. They do not seem to have been recorded hitherto.

Appendix A3 Application of isotopic mass scaling to transport properties

In order to test the quantitative consequences of the model defined by Eqs (6.4), (6.5) and (6.6), we consider in this Appendix a simple liquid metal with one ion-component. From Eq. (6.4) the Hamiltonian of the system is

$$H = \sum_{i=1}^{N_e} \frac{p_i^2}{2m} + \frac{1}{2} \sum_{i \neq j} \frac{e^2}{|\mathbf{r}_i - \mathbf{r}_j|} + \sum_{i=1}^{N_i} \frac{P_i^2}{2M} + \frac{1}{2} \sum_{i \neq j} W(|\mathbf{R}_i - \mathbf{R}_j|) + \sum_{i=1}^{N_e} \sum_{j=1}^{N_i} v(|\mathbf{r}_i - \mathbf{R}_j|) \tag{A3.1}$$

where

$$V(r) = a^{-1} \tilde{V}(ra^{-1}), \tag{A3.2}$$

$\tilde{V}(r)$ denoting the electron-fixed ion interaction potential. M is as usual the ion mass while $W(r)$ denotes the ion–ion interaction potential. At the densities appropriate to simple liquid metals, $W(r)$ is reasonably replaced by a Coulombic potential

$$W(r) = \frac{(ze)^2}{r} = a^{-1} W(ra^{-1}). \tag{A3.3}$$

In Eq. (A3.1), the ions are being treated classically, a good approximation above the melting point of metals.

Let us regard this Hamiltonian as a function of the dynamical variable sets p, r, P, R and parameters M, m and a. We express it formally as $H(p, r, P, R; M, m, a)$. We can easily show from Eqs (A3.1)–(A3.3) that this function has the following scaling property:

$$H(p, r, P, R; M, m, a) = a^{-1}H(pa, ra^{-1}, Pa, Ra^{-1}; Ma, ma, 1). \quad \text{(A3.4)}$$

Now we define H^* by

$$H^* = H(pa, ra^{-1}, Pa, Ra^{-1}; Ma, ma, 1). \quad \text{(A3.5)}$$

Equation (A3.4) suggests that the system defined by Eq. (A3.1), called below the H-system, has a definite relation to a system defined by Eq. (A3.5), called the H^*-system. It should be noted that in the H^* system the electron-ion interaction is not $V(r)$ but $\tilde{V}(ra^{-1})$. Let us introduce the following transformation t

$$t : (p, r, P, R, t, H) \to (p^*, r^*, P^*, R^*, t^*, H^*)$$

$$\text{by} \quad p^* = pa, r^* = ra^{-1}, P^* = Pa, R^* = Ra^{-1}, t^* = ta^{-1} \quad \text{and} \quad H^* = Ha. \quad \text{(A3.6)}$$

It is clear from the definition of t that it leaves the equations of motion invariant.

In what follows, we consider the application of the transformation above the mass scaling of thermodynamic quantities. Though we consider here the coefficient of self-diffusion D, the same discussion can also be applied to other transport coefficients. According to the Kubo formula for D

$$D = \pi \lim_{\omega \to 0} \omega^2 \lim_{k \to 0} \frac{1}{k^2} S_s(k, \omega) \quad \text{(A3.7)}$$

where

$$S_s(k, \omega) = \frac{1}{2\pi} \int \mathrm{d}t \exp(i\omega t) F_s(k, t), \quad \text{(A3.8)}$$

$$F_s(k, t) = \langle e^{i\mathbf{k}(\mathbf{R}_1(0) - \mathbf{R}_1(t))} \rangle_T, \quad \text{(A.39)}$$

$\langle \cdots \rangle_T$ being the canonical ensemble average in the H-system at temperature T.

By means of the transformation (A3.6) we can easily show that

$$F_s(k, t) \equiv f_s(k, t; M, m, T)$$
$$= f_s^*(k^*, t^*; M^*, m^*, T^*) \quad \text{(A3.10)}$$

where $k^* = ka$, $M^* = Ma$, $m^* = ma$, and $T^* = Ta$.

According to Eq. (A3.5), the interaction between an electron with mass m^* and ion with mass M^* as well as ion–ion interaction in the H^*-system does not depend on M^*. The thermodynamics of the ion-component in the system can be treated, as usual, as a quasi one-component system without further explicit reference to the electron degrees of freedom and the effective ion–ion interaction of the one-component system may be assumed to be independent of M^*. By following the discussion of Brown and March[34] we find

$$f_s^*(k^*, t^*; M^*, m^*, T^*) = \tilde{f}_s^*(k^*, M^{*-1/2}t^*; T^*, m^*). \tag{A3.11}$$

From Eqs (A3.7)–(A3.11):

$$D = \frac{a}{\sqrt{M^*}} h_s^*(T^*, m^*). \tag{A3.12}$$

As for the 'sound wave attenuation' $\frac{4}{3}\eta + \zeta$, η and ζ being shear and bulk viscosities respectively

$$\tfrac{4}{3}\eta + \zeta = \frac{\pi n M^2}{k_B T} \lim_{\omega \to 0} \omega^4 \lim_{k \to 0} \frac{1}{k^4} S(k, \omega) = \sqrt{M^*} h^*(T^*, m^*) \tag{A3.13}$$

It should be noted that unlike the classical mass scaling, temperature and electron-mass as well as ion mass are scaled in Eqs (A3.12) and (A3.13).

Let us test these mass-scaling laws by comparison with experimental data.[17,16] Since such data are clearly not available for the m^* dependence of h_s^* and h^*, we had no alternative but to assume this dependence can be neglected; this point requires further study in the future. From these equations we find the following mass scaling equations for liquid lithium

$$D^7(T) = \sqrt{\frac{M_6 a_7}{M_7 a_6}} D^6\left(\frac{a_7}{a_6} T\right) \tag{A3.14}$$

$$\eta^7(T) = \sqrt{\frac{M_7 a_7}{M_6 a_6}} \eta^6\left(\frac{a_7}{a_6} T\right), \tag{A3.15}$$

where

$$a_\alpha = 1 + \xi(m/M_\alpha)^k \tag{A3.16}$$

and we have assumed $\eta + \frac{3}{4}\zeta \simeq \eta$.

The parameter a is mainly determined by the short-range part of the electron-ion interaction in the liquid. This part of the interaction in the liquid would not be 'atom-like' but molecular-like or of multi-centre character. The departure of the parameter k from unity means the net effect of the ion movement on the electron-ion interaction. According to the Born–Oppenheimer approximation, the effect of the nuclear movement in a system of nuclei and electrons to its Hamiltonian appears in terms of the

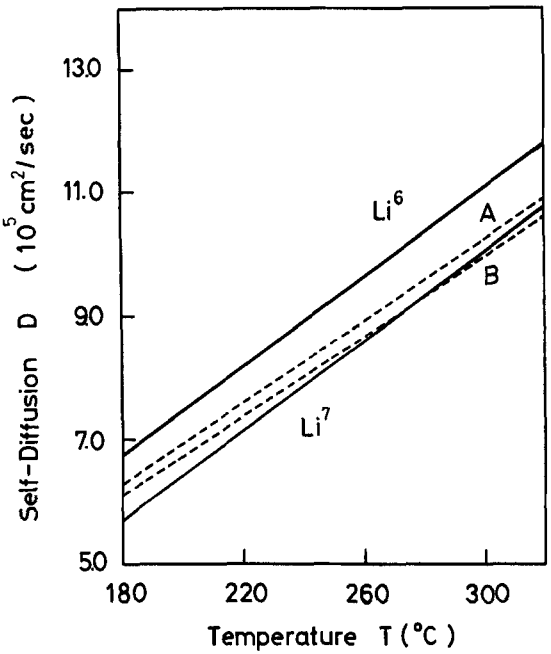

FIGURE A3.1 Temperature dependence of self-diffusion. Li^6 and Li^7 solid lines are given by Eq. (3.1), while the dashed lines are ealculated on the basis of Eqs. (A3.15), (A3.17) and Li^6 solid line. *A* is for $\xi = 0$ and *B* for $\xi = 10$ and $k = \frac{1}{4}$.

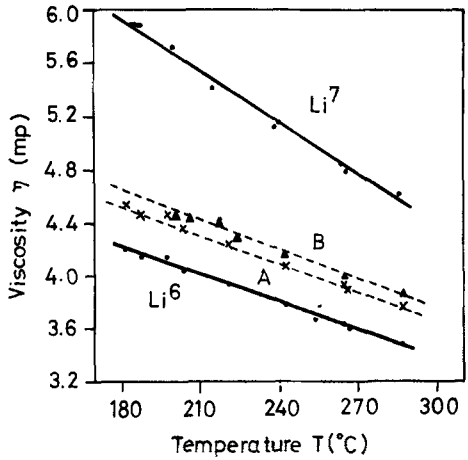

FIGURE A3.2 Temperature dependence of viscosity. Filled circles are the experimental data by Ban, Randall and Montgomery (1962), while crosses and filled triangles re calculated on the basis of Eqs (A3.16), (A3.17) and the experimental data for Li^6 and corresp ond to $\xi = 0$ and $\xi = 10$ with $k = \frac{1}{4}$, respectively.

power series expansion through $(m/M)^{1/4}$. Therefore a reasonable choice of k in Eq. (A3.16) may be equal to $\frac{1}{4}$.

Using this value plus Eqs. (A3.14) and (A3.15), we can obtain $D^7(T)$ and $\eta^7(T)$ for various values of ξ from experimental data of $D^6(T)$ and $\eta^6(T)$. The results are shown in Figures A3.1 and A3.2.

Though some departures of the kind required by experiment are displayed by the model, the departures remain too small to explain the experiments. Plainly, the model needs further refinement in the future.